Sound Transmission through Laminated Composite Cylindrical Shells, Considering Transverse Shear Deformation

K. Daneshjou[1], A. Nouri[2], and R. Talebitooti[3]
Mech. Eng. Dep't., Iran Univ. of Science and Tech.

ABSTRACT
Laminated composite shells are increasingly being used in various engineering applications, including aerospace, mechanical, marine, and automotive. In this paper, sound transmission through an infinite laminated composite cylindrical shell is studied in the context of the transmission of airborne sound into aircraft interior. The shell is immersed into an external fluid medium and contains internal fluid, while the airflow in external fluid medium is moving with a constant velocity. Modal impedance method, along with the first-order shear deformation theory (FSDT), is used to calculate the transmission loss (TL), considering three directions of the shell. The TL obtained in this study is compared with that of thin laminated composite obtained by others. The effects of structural properties and flight conditions on TL are studied for a range of values, especially, Mach number, aircraft flight altitude, shell thickness, and warp angle. Comparisons of the transmission loss are made among classical shell theory (CST) and FSDT for laminated composite and isotropic shells, which show close agreements.

Key Words: Wave Transmission Loss, Laminated Composite Shell, First-order Shear Deformation, Plane

انتقال صوت در پوسته‌های استوانه‌ای کامپوزیت لایه‌ای با در نظر گرفتن تغییر شکل برشی

کامران دانشجو، علی نوری و روح الله طالبی توتی
دانشکده مهندسی مکانیک، دانشگاه علم و صنعت ایران

چکیده
امروزه از پوسته‌های کامپوزیت لایه‌ای در کاربردهای مهندسی نظیر هوافضا، مکانیک، صنایع دریایی و خودرو به صورت گسترده‌ای استفاده می‌شود. در این مقاله، انتقال صوت به داخل یک پوسته کامپوزیت لایه‌ای نامحدود با هدف بررسی انتقال صوت به داخل کابین هواپیما مورد مطالعه قرار گرفته است. پوسته در داخل محیط سیال غوطه ور بوده و سیال خارجی با سرعت ثابت از روی آن عبور می‌کند. از روش امپیدانس مشخصه مودال و تئوری تغییر شکل برشی مرتبه اول برای محاسبه انتقال صوت با در نظر گرفتن سه جهت مختصات پوسته استفاده شده است. افت انتقال صوت بدست آمده در این مقاله با نتایج بدست آمده برای پوسته های جدار نازک کامپوزیت لایه‌ای توسط سایر محققین مقایسه شده است. همچنین، اثرات خواص سازه‌ای و شرایط پروازی، نظیر عدد ماخ، ارتفاع پرواز هواپیما، ضخامت جداره پوسته و زاویه چیدمان لایه‌ها بر افت انتقال صوت مورد بررسی قرار گرفته است. در پایان، نتایج افت انتقال صوت حاصل از تئوری کلاسیک پوسته و تئوری تغییر شکل برشی مرتبه اول برای پوسته‌های ایزوتروپ و کامپوزیت لایه‌ای با هم مقایسه شده‌اند.

واژه‌های کلیدی: افت انتقال، پوسته کامپوزیت لایه‌ای، تغییر شکل زاویه‌ای درجه ۱، موج صفحه‌ای

1- Associate Professor: kdaneshjo@iust.ac.ir

2- PhD Student (Corresponding Author): ali_nor@ mail.iust.ac.ir

3- PhD Student: rt_talebi@mail.iust.ac.ir

Introduction

Composite panels and cylinders are extensively employed in the aerospace industry. Their applications are commonly found in aircrafts, helicopters, launch vehicles and engine cowlings. Ironically, the light weight advantage of the composite construction could lead to higher interior noise levels. The prediction of the sound transmission into such structures requires the analysis of acoustic wave propagation in composite cylindrical shell. With the increase awareness of, and sensitivity to, structural noise and vibration, research covering the vibration of composite shells has received considerable attention.

Noise transmission, measured by transmission loss (TL) through the circular shell, has been studied by Smith [1], White [2], Koval [3-5], Blaise et al [6, 7] and Kim [8] for isotropic, orthotropic and laminated fiber-reinforced composite shells. Smith presented a theoretical study of transmission of sound energy through a thin, isotropic elastic cylindrical shell from an oblique plane wave excitation. White investigated sound transmission into finite cylindrical shells and found two important characteristics, the ring and coincidence frequencies, at which TL takes on minima. Koval extended Smith's work to present an analytical model for predicting of TL for isotropic, orthotropic, and laminated fiber-reinforced composite shells. The transmission loss prediction for orthotropic and multi-layered infinite cylinders was investigated in a series of papers by Blaise et al [6, 7]. They presented a displacement field which neglected the transverse shear and rotary inertia.

The theoretical study of Koval (1980), for an infinite cylindrical shell, provided the first model for noise transmission loss of composite constructions using classical laminated theory. Roussos et al. [9] gave a report prepared at the NASA Langley Research Centre about the theoretical and experimental study of noise transmission through composite plates. Tang et al. [10] considered an infinite cylindrical sandwich shell excited by an oblique plane sound wave with two independent incident angles. In most of studies surveyed above, numbers of terms used in the series solution were apparently insufficient to provide accurate results, which could have affected the very large TL's estimated results. In addition, the deformation of the transverse plane due to transverse shear stress was neglected, whereas in thick shells and in high frequency, transverse shear deformation could become important.

The objective of this paper is to study sound transmission through an infinite laminated composite cylindrical shell using "modal impedance method". An aircraft fuselage in flight with an external airflow is modelled as an infinite cylindrical shell. The vibro-acoustic model of laminated composite shell is obtained in a series form using FSDT laminated shell vibration, without ignoring any of the three directions of the shell. The shell is assumed to be immersed in a fluid media and excited by an incident oblique plane sound wave. The properties of the internal and external fluids surrounding the shell may be different. To make sure an enough number of modes are included in the analysis, the convergence checking is preformed. Moreover, the effects of structural properties and flight conditions on TL are studied for a range of values, especially, Mach number, flight altitude of aircraft and angle of warp. Comparison of TL is made between isotropic and composite shell using FSDT and CST.

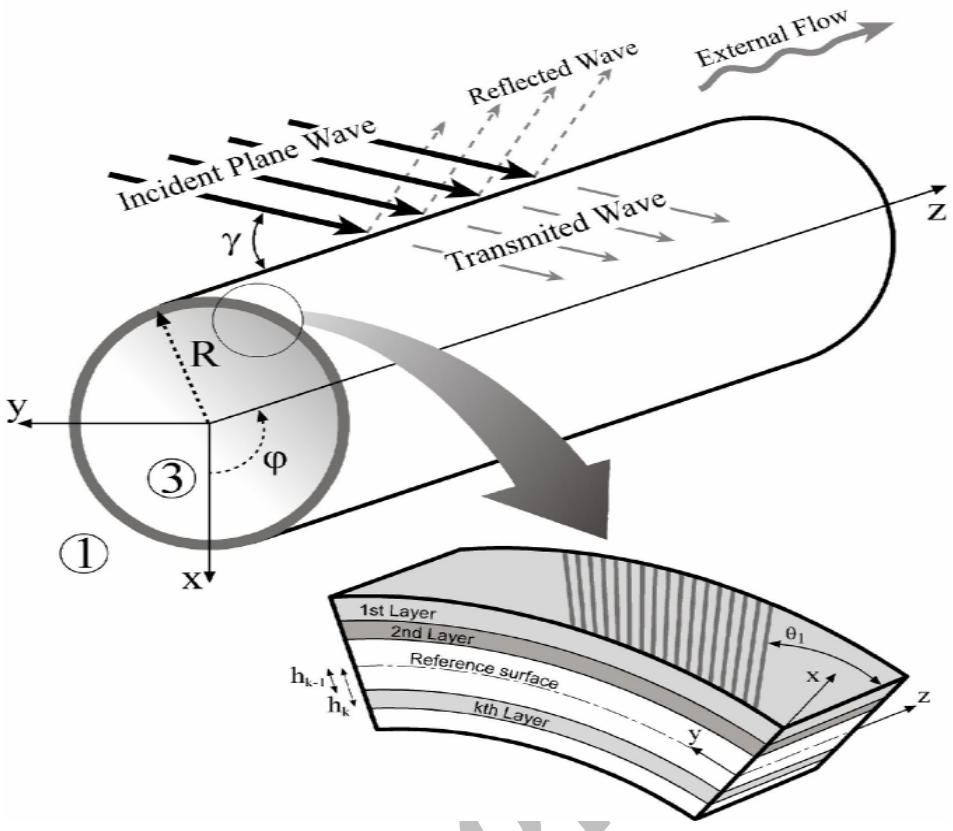

Fig. 1. Schematic diagram of the laminated composite cylindrical shell.

Model Specification

The specific problem consists of a plane sound wave obliquely impinging upon a flexible laminated composite shell, and includes the reflection and transmission of the incident wave, and the effect of an external airflow (see Figure 1). The wave approaches from the $\varphi = \pi$ direction with incident angle of γ. For mathematical simplicity the shell is considered to be of infinite length and the shell interior to be totally absorbing. The fluid media in the external and internal space are defined by the density and the speed of sound: $\{\rho_1, c_1\}$ and $\{\rho_2, c_2\}$ respectively.

Acoustic and Shell Dynamics

In the exterior space, the pressure $p_1 = p^I + p_1^R$, where p^I is the incident wave and p_1^R is the reflected wave, satisfies the convected wave equation (11, 12), as:

$$c_1^2 \nabla^2 \left(p^I + p_1^R\right) - \left(\frac{\partial}{\partial t} + V.\nabla\right)^2 (p^I + p_1^R) = 0, \quad (1)$$

where, ∇^2 is the Laplacian operator in the cylindrical coordinate system.

In the interior cavity, the pressure $p_3 = p_3^T$, where p_3^T is transmitted wave, satisfies the acoustic wave equation, as:

$$c_3^2 \nabla^2 p_3^T - \frac{\partial^2 p_3^T}{\partial t^2} = 0. \quad (2)$$

For the shell let $\{u_0, v_0, w_0\}$ be the displacements of the shell at the neutral surface in the axial, circumferential, and radial directions respectively, and $\{\psi_\alpha, \psi_\beta\}$ be the rotations of the normal direction relative to the unreformed mid-surface.

In FSDT, assuming that normal to the mid-surface strains remains straight during deformation but not normal to the mid-surface, the displacements can be written as [13, 14]:

$$\begin{aligned} u(\alpha,\beta,\xi) &= u_0(\alpha,\beta) + \xi.\psi_\alpha(\alpha,\beta), \\ v(\alpha,\beta,\xi) &= v_0(\alpha,\beta) + \xi.\psi_\beta(\alpha,\beta), \\ w(\alpha,\beta,\xi) &= w_0(\alpha,\beta), \end{aligned} \quad (3)$$

where, α and β are curvilinear surface coordinates and ξ is the distance from mid-surface. The middle surface strains and curvature change for a thick cylindrical shell are defined as:

$$\varepsilon_{0\alpha} = \frac{\partial u_0}{\partial \alpha}, \qquad \varepsilon_{0\beta} = \frac{\partial v_0}{\partial \beta} + \frac{w_0}{R},$$
$$\varepsilon_{0\alpha\beta} = \frac{\partial v_0}{\partial \alpha}, \qquad \varepsilon_{0\beta\alpha} = \frac{\partial u_0}{\partial \beta},$$
$$\gamma_{0\alpha\xi} = \frac{\partial w_0}{\partial \alpha} + \psi_\alpha,$$
$$\gamma_{0\beta\xi} = \frac{\partial w_0}{\partial \beta} - \frac{v_0}{R} + \psi_\beta, \qquad (4)$$
$$k_\alpha = \frac{\partial \psi_\alpha}{\partial \alpha}, \qquad k_\beta = \frac{\partial \psi_\beta}{\partial \beta},$$
$$k_{\alpha\beta} = \frac{\partial \psi_\beta}{\partial \alpha}, \qquad k_{\beta\alpha} = \frac{\partial \psi_\alpha}{\partial \beta}.$$

In above equation $\varepsilon_{0\alpha}$, $\varepsilon_{0\beta}$, $\varepsilon_{0\alpha\beta}$, $\varepsilon_{0\beta\alpha}$ are normal and shear mid-surface strains; $\gamma_{0\alpha\xi}$, $\gamma_{0\beta\xi}$ are shear strains in the z direction; k_α, k_β, $k_{\alpha\beta}$, $k_{\beta\alpha}$ are the curvature and twist changes. The subscript (0) refers to the middle surface in above equations.

The forces and moments resultant, obtained by integrating the stresses over the shell thickness, are:

$$\begin{bmatrix} N_\alpha \\ N_\beta \\ N_{\alpha\beta} \\ N_{\beta\alpha} \\ M_\alpha \\ M_\beta \\ M_{\alpha\beta} \\ M_{\beta\alpha} \end{bmatrix} = \begin{bmatrix} \overline{A}_{11} & A_{12} & \overline{A}_{16} & A_{16} & \overline{B}_{11} & B_{12} & \overline{B}_{16} & B_{16} \\ A_{12} & \hat{A}_{22} & A_{26} & A_{26} & B_{12} & \hat{B}_{12} & B_{12} & \hat{B}_{26} \\ \overline{A}_{16} & A_{26} & \overline{A}_{66} & A_{66} & \overline{B}_{16} & B_{26} & \overline{B}_{66} & B_{66} \\ A_{16} & \hat{A}_{26} & A_{66} & \hat{A}_{66} & B_{16} & \hat{B}_{26} & B_{66} & \hat{B}_{66} \\ \overline{B}_{11} & B_{12} & \overline{B}_{16} & B_{16} & \overline{D}_{11} & D_{12} & \overline{D}_{16} & D_{16} \\ B_{12} & \hat{B}_{22} & \hat{B}_{26} & \hat{B}_{26} & D_{12} & \hat{D}_{22} & D_{26} & \hat{D}_{26} \\ \overline{B}_{16} & B_{26} & B_{66} & B_{66} & \overline{D}_{16} & D_{26} & \overline{D}_{66} & D_{66} \\ B_{16} & \hat{B}_{26} & B_{66} & \hat{B}_{66} & D_{16} & \hat{D}_{26} & D_{66} & \hat{D}_{66} \end{bmatrix} \begin{Bmatrix} \varepsilon_{0\alpha} \\ \varepsilon_{0\beta} \\ \varepsilon_{0\alpha\beta} \\ \varepsilon_{0\beta\alpha} \\ \kappa_\alpha \\ \kappa_\beta \\ \kappa_{\alpha\beta} \\ \kappa_{\beta\alpha} \end{Bmatrix} \qquad (5)$$

$$\begin{bmatrix} Q_\alpha \\ Q_\beta \end{bmatrix} = \begin{bmatrix} A_{55} & A_{45} \\ A_{45} & A_{44} \end{bmatrix} \begin{bmatrix} \gamma_{0\alpha\xi} \\ \gamma_{0\beta\xi} \end{bmatrix}, \qquad (6)$$

where, N is membrane force resultant; M is moment resultant; Q_α, Q_β represent transverse shearing force resultants; A_{ij}, B_{ij} and D_{ij} are extensional, coupling and bending stiffness. For a composite shell composed of different orthotropic materials the stiffness can be written as [13]:

$$\left.\begin{aligned} A_{ij} &= \sum_{k=1}^{N_L} \overline{Q}_{ij}^{k} (h_k - h_{k-1}) \\ B_{ij} &= \frac{1}{2} \sum_{k=1}^{N_L} \overline{Q}_{ij}^{k} (h_k^2 - h_{k-1}^2) \\ D_{ij} &= \frac{1}{3} \sum_{k=1}^{N_L} \overline{Q}_{ij}^{k} (h_k^3 - h_{k-1}^3) \end{aligned}\right\} \quad i,j = 1,2,6, \qquad (7)$$

$$\left.\begin{aligned} A_{ij} &= \sum_{k=1}^{N_L} K_i K_j \overline{Q}_{ij}^{k} (h_k - h_{k-1}) \\ B_{ij} &= \frac{1}{2} \sum_{k=1}^{N_L} K_i K_j \overline{Q}_{ij}^{k} (h_k^2 - h_{k-1}^2) \\ D_{ij} &= \frac{1}{3} \sum_{k=1}^{N_L} K_i K_j \overline{Q}_{ij}^{k} (h_k^3 - h_{k-1}^3) \end{aligned}\right\} \quad i,j = 4,5, \qquad (8)$$

where, h_{k-1} and h_k denote the distances from the reference surface to the outer and inner surfaces of the kth layer as shown in Fig. 1, N_L is the number of layers in the laminated shell and $K = \sqrt{5/6}$ is shear correction coefficient [13- 15].

In both of equations (7, 8) the constants $\overline{Q}_{ij}$ are transformed stiffness coefficients, which are found from the following equation:

$$[\overline{Q}] = [T]^{-1}[Q][T], \qquad (9)$$

where, [T] is the transformation matrix for principal material coordinate and shell coordinates system and defined as:

$$[T] = \begin{bmatrix} \cos^2\theta_k & \sin^2\theta_k & 2\cos\theta_k \sin\theta_k \\ \sin^2\theta_k & \cos^2\theta_k & -2\cos\theta_k \sin\theta_k \\ -\cos\theta_k \sin\theta_k & \cos\theta_k \sin\theta_k & \cos^2\theta_k - \sin^2\theta_k \end{bmatrix} \qquad (10)$$

In addition θ_k is orientation of fibres and Q_{ij} are material constants that were defined in terms of material properties of the orthotropic ply, as:

$$Q_{11} = E_1 \frac{1}{\Delta}, \qquad Q_{22} = E_2 \frac{1}{\Delta}, \qquad (11)$$

$$Q_{66} = G_{12}, \qquad Q_{12} = E_1 \frac{\nu_{21}}{\Delta} = E_2 \frac{\nu_{12}}{\Delta},$$
$$\Delta = 1 - \nu_{12}\nu_{21},$$

where, E_1 and E_2 are modulus of elasticity in the 1 and 2 directions, respectively; G_{12} is modulus of

shear stiffness and $\nu_{ij}(i,j=1,2,i\neq j)$ are Poisson's ratios.

Note that we described the fiber coordinates of orthotropic, as 1 and 2, where direction 1 is parallel to the fibers and 2 is perpendicular to them.

Considering first-order shear deformation theory, the equations of motion of the laminated composite cylindrical shell are defined as [13, 14]:

$$\frac{\partial N_{\alpha}}{\partial \alpha}+\frac{\partial N_{\alpha\beta}}{\partial \beta}+q_{\alpha}=(\bar{I}_1\ddot{u}_0^2+\bar{I}_2\ddot{\psi}_{\alpha}^2), \quad (12)$$

$$\frac{\partial N_{\beta}}{\partial \beta}+\frac{\partial N_{\alpha\beta}}{\partial \alpha}+\frac{Q_{\beta}}{R}+q_{\beta}=(\bar{I}_1\ddot{v}_0^2+\bar{I}_2\ddot{\psi}_{\beta}^2) \quad (13)$$

$$-\frac{N_{\beta}}{R}+\frac{\partial Q_{\alpha}}{\partial \alpha}+\frac{\partial Q_{\beta}}{\partial \beta}+q_{\xi}=(\bar{I}_1\ddot{w}_0^2), \quad (14)$$

$$\frac{\partial M_{\alpha}}{\partial \alpha}+\frac{\partial N_{\beta\alpha}}{\partial \beta}-Q_{\alpha}+m_{\alpha}=(\bar{I}_2\ddot{u}_0^2+\bar{I}_3\ddot{\psi}_{\alpha}^2), \quad (15)$$

$$\frac{\partial M_{\beta}}{\partial \beta}+\frac{\partial N_{\alpha\beta}}{\partial \alpha}-Q_{\beta}+m_{\beta}=(\bar{I}_2\ddot{v}_0^2+\bar{I}_3\ddot{\psi}_{\beta}^2). \quad (16)$$

Equation. (12-14) present the equation of the translation motion and Equation. (15, 16) present the equations of rotational motion. In above equations q_{α}, q_{β} and q_{ξ} are external forces (per unit area) in the α,β and ξ directions, respectively, m_{α} and m_{β} represent distributed couples about the middle surface of the shell (per unit length) and two dots represent the second derivative of these terms with respect to time, and:

$$\bar{I}_i=\left(I_i+\frac{I_{i+1}}{R}\right) \quad i=1,2,3, \quad (17)$$

$$I_i=\sum_{k=1}^{N_L}\int_{-h/2}^{h/2}\rho_k\,\xi^{i-1}\,d\xi \quad i=1,2,3,4, \quad (18)$$

where, ρ_k is the mass density of *k*-th layer. For cylindrical shells in Fig. 1, $\beta=R\varphi$ and $\alpha=z$, therefore the equations of motion can be written in terms of displacements [13, 15], as:

$$[L]\{u\}+[M]\{\ddot{u}\}=\{q\}, \quad (19)$$

where,

$$\{u\}=\left[u_o, v_0, w_0, \psi_z, \psi_{\varphi}\right]^T, \quad (20)$$

$$[M]=\begin{bmatrix}\bar{I}_1 & 0 & 0 & \bar{I}_2 & 0\\ 0 & \bar{I}_1 & 0 & 0 & \bar{I}_2\\ 0 & 0 & \bar{I}_1 & 0 & 0\\ \bar{I}_2 & 0 & 0 & \bar{I}_3 & 0\\ 0 & \bar{I}_2 & 0 & 0 & \bar{I}_3\end{bmatrix}, \quad (21)$$

and

$$\{q\}=\left[0,0,\left(p_1^I+p_1^R\right)-p_3^T,0,0\right]^T. \quad (22)$$

The L_{ij} coefficients are shown in appendix A. In addition, the classical equations of thin laminated composite shell can be found in appendix B [15, 16].

Boundary Conditions

We have to consider, for a coupled fluid-structure problem, the boundary conditions at internal and external shell surfaces. On the internal and external shell surfaces, the particle velocities of the acoustic media in the normal direction have to be equal to the normal velocity of the shell. These results are shown in the following equations [11, 17]:

$$\left.\frac{\partial(p^I+p_1^R)}{\partial r}\right|_{r=R}=-\rho_1\left(\frac{\partial}{\partial t}+V.\nabla\right)^2 w, \quad (23)$$

$$\left.\frac{\partial p_3^T}{\partial r}\right|_{r=R}=-\rho_3\frac{\partial^2 w}{\partial t^2}, \quad (24)$$

which describe the effect of the fluid pressure on the shell motion.

Solution of the Vibro-acoustic Equations

The harmonic plane wave p^I in cylindrical geometry, incident from outside to the direction shown in Fig. 1, can be expressed as [6, 8, 18]:

$$p^I(r,z,\theta,t)=P_0\sum_{m=0}^{\infty}\varepsilon_m(-j)^m J_m(k_{1r}r)e^{[j(\omega t-k_{1z}z-m\varphi)]}, \quad (25)$$

where, ε_m is the Neumann factor given by:

$$\varepsilon_m=\begin{cases}1 & m=0,\\ 2 & m\geq 1,\end{cases} \quad (26)$$

and

$$k_{1z}=k_1\cos\gamma, \quad k_{1r}=k_1\sin\gamma. \quad (27)$$

In addition k_1 is the wave number in the moving medium and J_m is the Bessel function of the first kind of order m, p_0 is the amplitude of the incident wave, $j=\sqrt{-1}$, m=0,1,2,3, . . . and ω is the angular frequency.
The wave number in moving medium can be written as [3]:

$$k_1 = \frac{\omega}{c_1}\left(\frac{1}{1+M_1\cos\gamma}\right), \quad (28)$$

where, $M_1 = (V/c_1)$ is the Mach number of the external flow.
Because the travelling waves in the acoustic media and inside the shell are driven by the incident-travelling wave, the wave numbers (or trace velocities) in the z direction should match throughout the system, therefore $k_{3z} = k_{1z}$ and:

$$k_3 = \frac{\omega}{c_3}\ , \quad k_{3z} = k_{1z}\ , k_{3r} = \sqrt{k_3^2 - k_{3z}^2}\ . \textbf{(29)}$$

The waves radiated from the shell to the outside and into the cavity, p_1^R and p_3^T, can be represented as:

$$p_1^R(r,z,\theta,t) = \sum_{m=0}^{\infty} P_{1m}^R\, H_m^2(k_{1r}r)\, e^{[j(\omega t - k_{1z}z - m\varphi)]}\ , \quad (30)$$

$$p_3^T(r,z,\theta,t) = \sum_{m=0}^{\infty} P_{3m}^T\, H_m^1(k_{3r}r)\, e^{[j(\omega t - k_{1z}z - m\varphi)]}\ , \quad (31)$$

where, H_m^1 and H_m^2 are the Hankel functions of the first and second kind of order m, respectively. The former represents the incoming wave and the latter the outgoing wave. The displacement and rotation terms of mid surface can be written as follows:

$$\begin{Bmatrix} u_0 \\ v_0 \\ w_0 \\ \psi_{0z} \\ \psi_{0\theta} \end{Bmatrix} = \sum_{m=0}^{\infty} \begin{Bmatrix} jU_m \\ jV_m \\ W_m \\ j\psi_{zm} \\ j\psi_{\varphi m} \end{Bmatrix} e^{[j(\omega t - k_{1z}z - m\varphi)]}. \quad (32)$$

Here, in Equation. (32), $\{U_m, V_m, W_m\}$ and $\{\psi_{zm}, \psi_{\varphi m}\}$ are unknown complex amplitudes of the displacement and rotation components, respectively. It can be seen that for each mode number *m*, there are seven unknowns $\{U_m, V_m, W_m, \psi_{zm}, \psi_{\varphi m}, P_{1m}^R, P_{3m}^T\}$ and seven equations (five equation of motion and two boundary condition). To obtain simplified and meaningful results, one can get a set of equations in terms of P_{1m}^R, P_{3m}^T and W_m by eliminating $U_m, V_m, \psi_{zm}, \psi_{\varphi m}$. Solving these coupled equations yields:

$$P_{1m}^R = -P_0\varepsilon_m(-j)^m \frac{J_m'(k_{1r}R)}{H^{2\prime}(k_{1r}R)} \frac{(Z_m^T + Z_m^I + Z_m^{Sh})}{Z_m^T + Z_m^R + Z_m^{Sh}}, \quad (33)$$

$$P_{3m}^T = -P_0\varepsilon_m(-j)^m \frac{-\rho_2 k_{1r} J_m'(k_{1r}R) Z_m^R + Z_m^I (k_1 c_1/\omega)^2}{\rho_1 k_{3r} H^{1\prime}(k_{3r}R)(Z_m^R + Z_m^T + Z_m^{Sh})}, \quad (34)$$

$$W_m = -P_0\varepsilon_m(-j)^m \frac{k_{1r} J_m(k_{1r}R) Z_m^R + Z_m^I (k_1 c_1/\omega)^2}{\rho_1\omega^2 (Z_m^R + Z_m^T + Z_m^{Sh})}, \quad (35)$$

where ,

$$Z_m^I = i\omega\frac{\rho_1}{k_{1r}}\frac{J_m(k_{1r}R)}{J_m'(k_{1r}R)}, \quad (36)$$

$$Z_m^R = -i\omega\frac{\rho_1}{k_{1r}}\frac{H^2(k_{1r}R)}{H^{2\prime}(k_{1r}R)}\left(\frac{k_1 c_1}{\omega}\right)^2, \quad (37)$$

$$Z_m^T = i\omega\frac{\rho_2}{k_{2r}}\frac{H^1(k_{3r}R)}{H^{1\prime}(k_{3r}R)}, \quad (38)$$

$$Z_m^{Sh} = \frac{P_0\varepsilon_m(-j)^m J_m(k_{1r}R) + P_m^R H^2(k_{1r}R) - P_{3m}^T H^1(k_{3r}R)}{j\omega W_m} = \frac{1}{j\omega D_m}. \quad (39)$$

Here, in Equation. (33) to (39), the primes denote derivatives with respect to the argument; Z_m^I, Z_m^R, Z_m^T are modal characteristic acoustic impedances of the fluids; Z_m^{sh} is the modal impedance of the shell; and D_m is the modal amplitude of the displacement component of the shell in the radial direction with a unit pressure.

Transmission Loss

It is convenient to represent the solution in TL for the design purpose. TL can be defined as the ratio of the incoming and transmitted sound powers per unit length of the cylinder [6, 8], as:

$$TL = 10\log_{10}\frac{W^{I}}{W^{T}}, \quad (40)$$

where, W^{I} is the incident power and W^{T} is the transmitted power per unit length of the shell [8], as:

$$W^{I} = \frac{\cos\gamma\, P_0^2}{\rho_1 c_1} \times R, \quad (41)$$

$$W^{T} = \frac{1}{2}\mathrm{Re}\left\{\int_0^{2\pi} p_3^{T}.\partial/\partial t\,(w_0)^{*}\, r\, d\varphi\right\}, \; r = R, \quad (42)$$

where, Re {.} and the superscript $*$ represent the real part and the complex conjugate of the argument, respectively. Substituting Equation (31, 32) by using Equation. (33, 35) into Equation (40) leads to the expression of TL in terms of the modal impedances, as:

$$TL = -10\log_{10}\sum_{m=0}^{\infty}\frac{2\varepsilon_m}{k_{1r}R}\left(\frac{\omega}{k_1 c_1}\right)^{*}\frac{\mathrm{Re}[Z_m^{R}]+\mathrm{Re}[Z_m^{T}]}{\left|Z_m^{R}+Z_m^{T}+Z_m^{Sh}\right|^2}, \quad (43)$$

where, $|.|$ is the absolute value of the argument.

In addition, the average power transmission coefficient $\bar{\tau}$ is given as [19]:

$$\bar{\tau} = \int_{\gamma_{min}}^{\gamma_{max}} \tau(\gamma)\sin\gamma\cos\gamma\, d\gamma, \quad (44)$$

where, $\tau(\gamma)$ is the power transmission coefficient calculated for the incident angle γ; γ_{min} and γ_{max} are the critical angles of incidence upon the shell [3]. Incidence wave out of this range, to be totally scattered with no transmission into the shell interior.

The integration in Eq. (44) is conducted numerically by the Simpson's rule using an integration step-size of 2° [20]. The average TL_{av} shown in Fig. 2. is given as [21]:

$$TL_{av} = 10\log_{10}\left(\frac{1}{\bar{\tau}}\right). \quad (45)$$

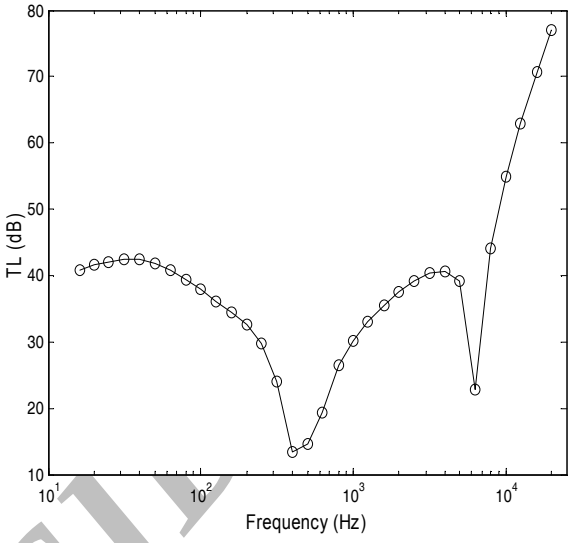

Fig. 2. TL averaged for random incident angles.

Convergence checking

As one can see in Equation. (25) and (30–32), the solutions, are obtained in series form. Therefore, one has to ensure that enough number of modes are included in the analysis to make the solution converge. When insufficient number of modes is used in the calculation, the resulting TL becomes overestimated. Once the solution converges at a given frequency, it can be assumed to converge in all frequencies lower than that, because more terms are necessary to be used in the calculation for a higher frequency. Therefore, we construct an iterative procedure in each frequency, considering the maximum iteration number. Unless the convergence condition is met, it iterates again. When the TL's calculated at two successive calculations are within a pre-set error bound, the solution is considered to have converged. Fig. 3 shows the concept of this convergence. Changes in the calculated TL as the number of modes increases are shown in Fig. **4** for the case of a composite shell specified in table 1 driven at 1000 Hz. Fig. 5 shows the convergence trend for the same case but at 10,000 Hz, which indicates that with increasing the frequency, the number of modes for convergence is increased.

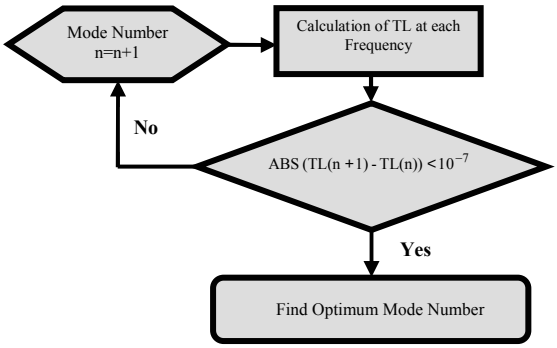

Fig. 3. Algorithm for identifying the optimum mode number.

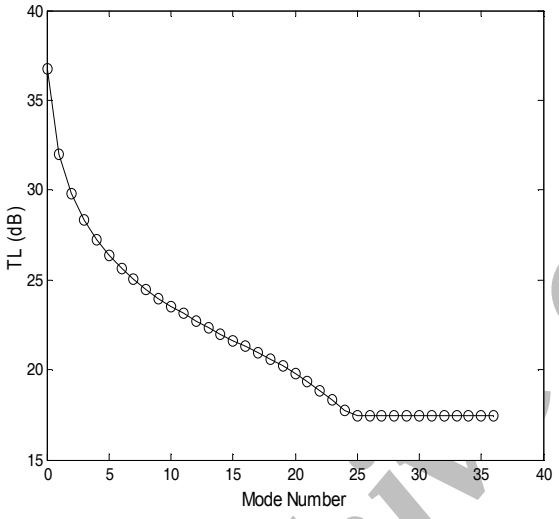

Fig. 4. Mode convergence diagram for 10-layers laminated composite at 1000 Hz.

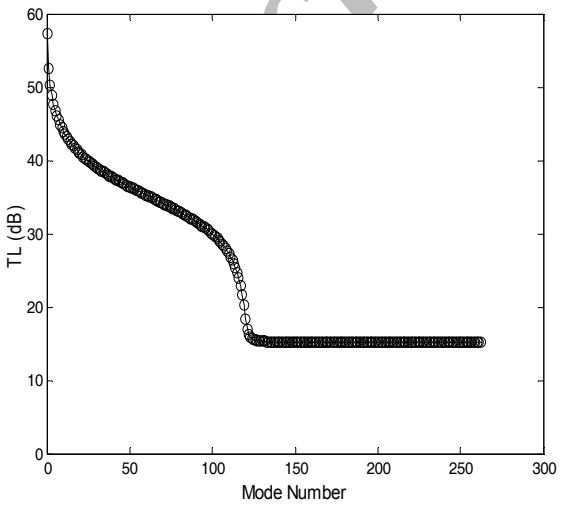

Fig. 5. Mode convergence diagram for the 10-layers composite shell at 10000 Hz.

Table1. Geometrical and environmental properties.

	Shell		Cavity	Ambient
Material (Fluid)	Al	G/E	Air	Air
Density (kg/m^3)	2760	1600	1.21	1.21
E_1 **(GPa)**	71	138	-	-
E_2 **(GPa)**	71	8.9	-	-
G_{12} **(GPa)**	27.7	7.1		
G_{13} **(GPa)**	27.7	7.1		
G_{23} **(GPa)**	27.7	6.2		
$\nu_{z\theta}$	0.3	0.26	-	-
Sound Speed (m/s)	5316	5622	343	343
Incidence Angle	45			

Numerical result

Numerical results have been generated for geometry typical of a narrow-bodied jet fuselage made of the laminated composite shell with radius R=1.83 m and total thickness h=1.59 mm. Both internal and external fluids are considered at sea level conditions, and its external flow Mach number is assumed as $M_1 = 0$ for the purpose of this study, except where noted. In addition each layer of the composite shell is made of Graphite/Epoxy (table 1). The plies are arranged in a $[0^\circ,90^\circ,45^\circ,-45^\circ,0^\circ]_S$ pattern. Comparison of the transmission loss is made among classical shell theory (CST) and FSDT for composite and isotropic shells. The basic shell dimensions and simulation conditions used in the study are listed in Table 1. Parametric numerical studies of transmission loss (TL) are conducted for broadband frequency. These studies provide insight into the effect of the acoustic properties of the fluids and the structural or material parameters of the shells on TL. The theoretical model developed can be used very effectively in the basic design stage of cylinder-shape vibro-acoustic systems and show the effect of the acoustic properties of the fluids and the structural parameters on TL.

Fig. **6** shows a comparison on TL for the thin shell theory purposed by Koval [5] and the first-order shell theory presented in this study. As shown, three important frequencies are recognized: ring frequency f_r (where the wavelength of a longitudinal wave in the shell equal to the circumference), critical pseudo-coincidence

f_{pc} (spatial coincidence in radial direction between the wave vector projection of excitation and the shell circumferential wave number) and coincidence frequency f_c (where the trace velocity of the acoustic wave is equal to the bending wave velocity in the shell wall). The various zones controlled by the stiffness $(0 - f_r)$, the mass $(f_r - f_{pc})$ and the coincidence $(f > f_c)$ and the resonant modes zone enclosed between f_{pc} and f_c will be noted. At the lower frequency, the effects of shear and rotation on TL are negligible. However, in the high frequency range, the shear waves transmit sound through the shell resulting in a decrease of TL. Thus, the use of FSDT is strongly recommended for high frequencies.

Different ambient conditions are considered here table 2. A higher flight altitude, affecting on density and sound velocity of fluid, will lead to a larger acoustic impedance mismatch between the fluids inside and outside the shells. As shown in Fig. 7, increasing of acoustic mismatch makes the TL increases in broadband of frequency. For instance in some region it may be enhanced more than 10dB.

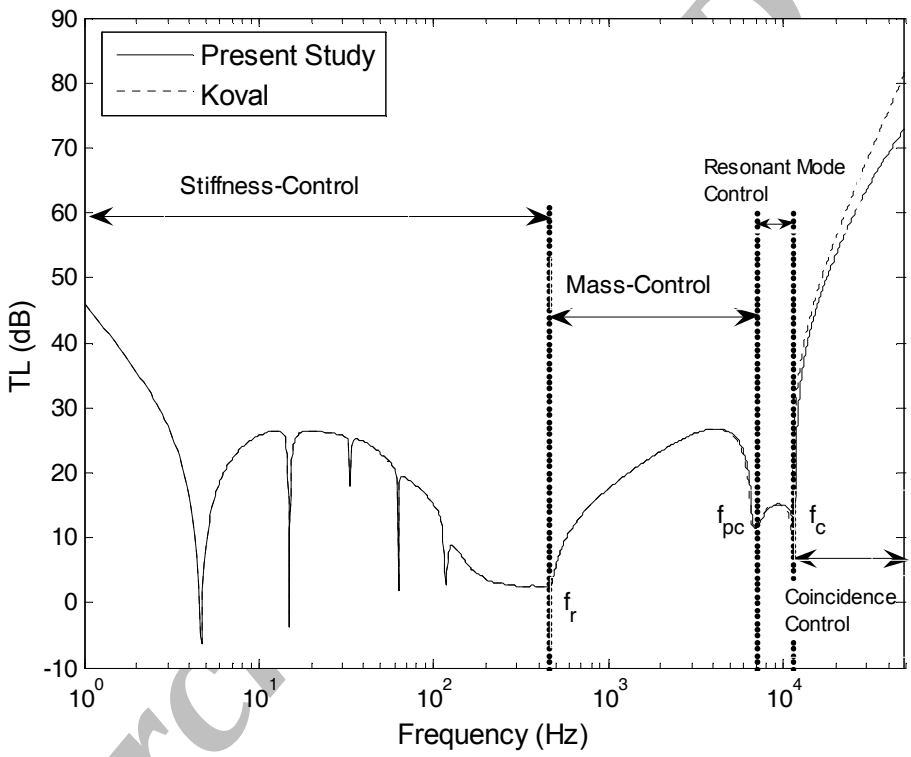

Fig. 6. Comparison of Presented study with Koval 10-layeres composite shell.

Table 2- Flight conditions.

Name	1st Cond.	2nd Cond.	3rd Cond.
Altitude (m)	3050	7600	10650
$\rho\ (kg/m^3)$	0.9041	0.5489	0.379
c (m/s)	328.55	309.96	296.5

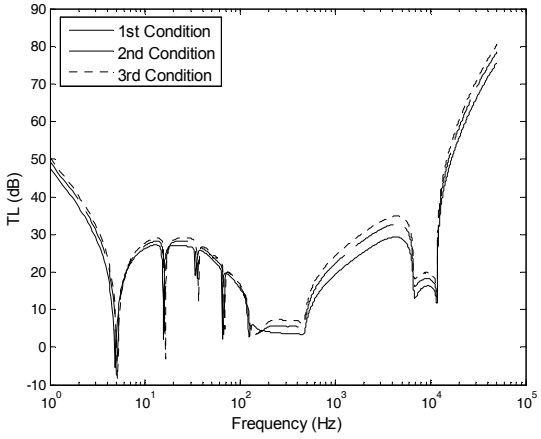

Figure 7. TL curves for three ambient conditions.

External airflow influences the axial and radial wave numbers; thus, the TL will be changed due to this effect. Fig. 8, shows the effects of Mach numbers with M = 0, 0.5, and 1.0, on TL. With increasing Mach number, the TL is descending in stiffness-controlled region (below the ring frequency), whereas in upper frequency more than ring frequency it is ascending. Also, the coincidence frequency is shifted upwards with increase of Mach number.

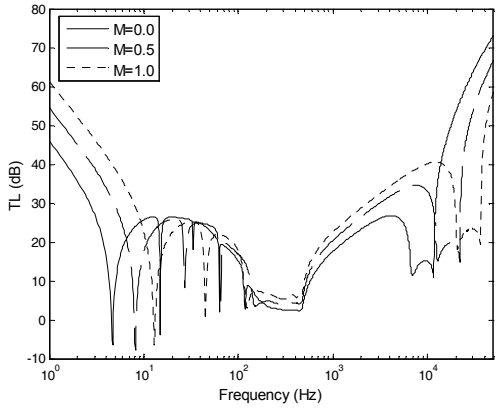

Fig. 8. TL curves for 10-layered laminated shell subjected in uniform flow.

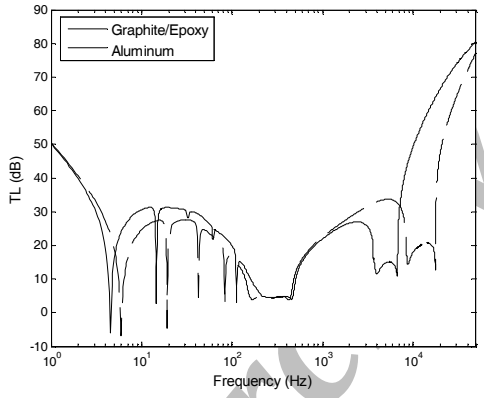

Fig. 9. Comparison between Aluminium and 10-layers laminate composite shell.

Fig. 9 shows a comparison between the cylinder transmission loss for an aluminium shell and a 10-layered composite shell of same weight. The figure indicate that the ring frequency is shifted upwards, so that there appear to be a gain in TL below the ring frequency, but composite shell does not appear to be effective as an aluminium shell above the ring frequency. This appear to be due to the fact that the critical frequency of a composite shell is lower than it is for an aluminium shell, so that the TL curve is never able to reach a full mass law behaviour because the ring frequency and the critical frequency are closer together. It thus appears that a composite shell does not appear to offer significant advantages over an aluminium shell, as regards noise attenuation.

Fig. 10, shows the effect on TL of the angle of warp, θ_k of the individual layers of the composite shell. In this Figure, all of the layers have the same angle θ_k. The individual curves in Fig.10 Correspond to $\theta_k = 0^\circ, 30^\circ, 45^\circ, 60^\circ, 90^\circ$. The incidence angle of the incident plane wave is $\theta = 30^\circ$. The results shown in the curve indicate that the noise attenuation of a composite shell is sensitive to the angle of warp and suggests the possibility of tailoring a composite shell a specific need.

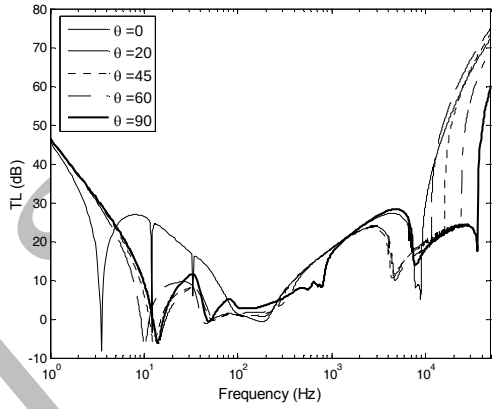

Fig. 10. Effect of fibre orientation on TL, at $\gamma = 30^\circ$ for a 10-layered composite shell.

Fig. 11 shows the effect of the composite material on TL. Materials chosen for the comparison are Graphite/Epoxy, Glass/ Epoxy and Boron/Epoxy as shown in table (3). The figure shows that material must be chosen properly to enhance TL at stiffness-controlled zone. The best result is obtained from Boron/Epoxy shell, which represents a desirable level of TL at stiffness-control zone. It is readily seen that, in higher frequency, because of density of materials, the TL curves are ascending. Therefore the TL of Glass/Epoxy is higher than the other materials in mass-controlled region.

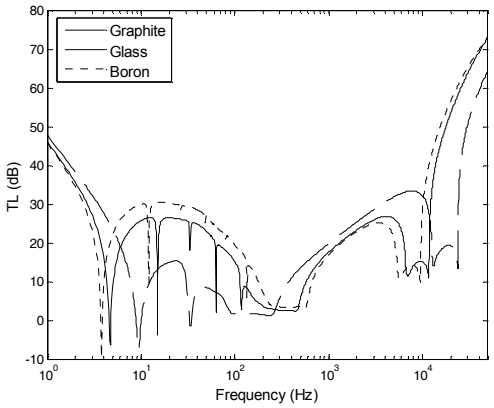

Fig. 11. TL curves for 10-layers laminated composite shell with different material.

Table3. Composite materials properties.

Material	Graphite /Epoxy	Glass/ Epoxy	Boron/ Epoxy
ρ (kg/m^3)	1600	1900	1600
E_1 **(GPa)**	138	38.6	206
E_2 **(GPa)**	8.9	8.2	20.6
G_{12} **(GPa)**	7.1	4.2	6.89
G_{13} **(GPa)**	7.1	4.2	6.89
G_{23} **(GPa)**	6.2	3.45	4.1
ν_{12}	0.3	0.26	0.3

To properly reveal the effects of shear deformation, a comparison between CST & FSDT is made for two different shell thicknesses of h=1.59mm and h=4.77mm in Fig. 12. As shown, with increasing of shell thickness, the difference between CST and FSDT is increased in high frequency. It appears that, the effects of shear deformation on sound transmission are increased when the wave length are short enough i.e.; of the same order or less than the thickness of the shell.

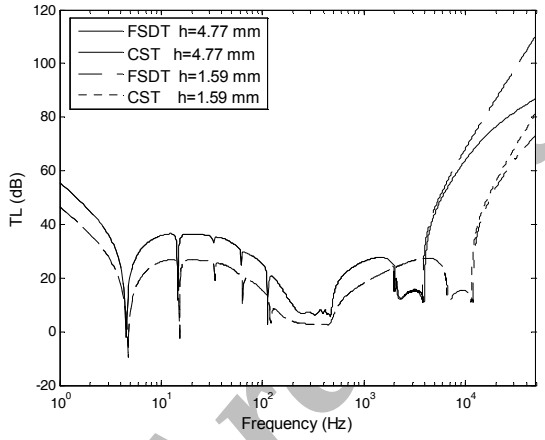

Fig. 12. Comparison of CST & FSDT in two different shell thicknesses.

Figure 13 shows a comparison for the same radius and thickness composite and aluminium shells using both FSDT and CST. At the lower frequency, the effects of shear on TL are negligible. However, in the high frequency range, the shear waves transmit sound through the shell resulting in a decrease of TL. Tabular data is also generated Table 4. The results show that, the difference between FSDT and CST for laminated composite shell is more than that of aluminium shell. It would appear that, the effect of shear deformation on sound transmission for composite becomes more important than aluminum shell. Therefore, the use of FSDT theory is suggested for composite shell.

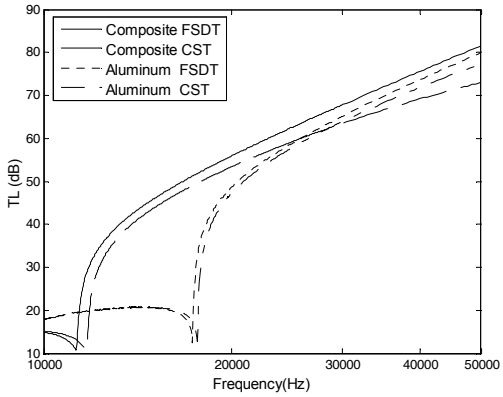

Figure 13. Comparison of CST & FSDT for aluminium and composite shells.

Table4. Comparison of FSDT and CST for composite and aluminium shell

Frequency (Hz)	Transmission Loss			
	Composite		Aluminium	
	FSDT	CST	FSDT	CST
10	25.63	25.63	24.36	24.36
100	15.05	15.05	15.89	15.89
1000	17.42	17.42	22.26	22.26
5000	26.28	26.11	32.55	32.50
10000	15.09	14.85	18.99	19.09
20000	53.43	55.96	53.17	54.22
30000	63.45	67.78	66.57	68.04
40000	69.19	75.63	74.03	76.31
50000	73.00	81.58	79.18	82.43

Conclusions

In this paper, sound transmission through an infinite laminated composite cylindrical shell has been studied. A modal impedance method is used to obtain TL, including the effect of the external airflow. The frequency spectrum of TL is studied by varying parameter of fluids and shells. The following conclusions can be drawn from this numerical study:

1- In higher altitude, acoustic impedance mismatch increases. Therefore, TL in all frequency bands is enhanced.

2- By increasing Mach number, the TL is descending in stiffness-controlled region and the coincidence frequency is shifted upward.

3- Comparison between aluminium and laminated composite shell is done. It appears composite shell to be a gain in TL below the ring frequency, but composite shell does not appears to be effective as an aluminium shell above the ring frequency.

4- The noise attenuation of a composite shell is sensitive to the angle of warp of layers.

5- Since, the effect of shear waves on sound transmission for composite becomes more important than aluminum shell, the use of FSDT theory is strongly recommended for composite shell.

Appendix A

The L_{ij} coefficients are given below

$$L_{11} = \bar{A}_{11}\frac{\partial^2}{\partial z^2} + \frac{2A_{16}}{R}\frac{\partial^2}{\partial z\partial\varphi} + \frac{\hat{A}_{66}}{R^2}\frac{\partial^2}{\partial\varphi^2} - \bar{I}_1\frac{\partial^2}{\partial t^2}$$

$$L_{12} = \bar{A}_{16}\frac{\partial^2}{\partial z^2} + \frac{A_{12}+A_{66}}{R}\frac{\partial^2}{\partial z\partial\varphi} + \frac{\hat{A}_{26}}{R^2}\frac{\partial^2}{\partial\varphi^2},$$

$$L_{13} = \frac{A_{12}}{R}\frac{\partial}{\partial z} + \left[\frac{\hat{A}_{26}}{R^2}\right]\frac{\partial}{\partial\varphi},$$

$$L_{14} = \bar{B}_{11}\frac{\partial^2}{\partial z^2} + \frac{2B_{16}}{R}\frac{\partial^2}{\partial z\partial\varphi} + \frac{\hat{B}_{66}}{R^2}\frac{\partial^2}{\partial\varphi^2} - \bar{I}_2\frac{\partial^2}{\partial t^2},$$

$$L_{15} = \bar{B}_{16}\frac{\partial^2}{\partial z^2} + \frac{B_{12}+B_{66}}{R}\frac{\partial^2}{\partial z\partial\varphi} + \frac{\hat{B}_{26}}{R^2}\frac{\partial^2}{\partial\varphi^2},$$

$$L_{22} = \bar{A}_{66}\frac{\partial^2}{\partial z^2} + \frac{2A_{26}}{R}\frac{\partial^2}{\partial z\partial\varphi} + \frac{\hat{A}_{22}}{R^2}\frac{\partial^2}{\partial\varphi^2} - \frac{\hat{A}_{44}}{R^2} - \bar{I}_1\frac{\partial^2}{\partial t^2}$$

$$L_{23} = \frac{A_{26}+A_{45}}{R}\frac{\partial}{\partial z} + \frac{\hat{A}_{22}+\hat{A}_{44}}{R^2}\frac{\partial}{\partial\varphi},$$

$$L_{24} = \bar{B}_{16}\frac{\partial^2}{\partial z^2} + \frac{B_{12}+B_{66}}{R}\frac{\partial^2}{\partial z\partial\varphi} + \frac{\hat{B}_{26}}{R^2}\frac{\partial^2}{\partial\varphi^2} + \frac{A_{45}}{R},$$

$$L_{25} = \bar{B}_{66}\frac{\partial^2}{\partial z^2} + \frac{2B_{26}}{R}\frac{\partial^2}{\partial z\partial\varphi} + \frac{\hat{B}_{22}}{R^2}\frac{\partial^2}{\partial\varphi^2} + \frac{\hat{A}_{44}}{R^2} - \bar{I}_2\frac{\partial^2}{\partial t^2}$$

$$L_{33} = -A_{55}\frac{\partial^2}{\partial z^2} - \frac{2A_{45}}{R}\frac{\partial^2}{\partial z\partial\varphi} - \frac{\hat{A}_{44}}{R^2}\frac{\partial^2}{\partial\varphi^2} + \frac{\hat{A}_{22}}{R^2} - \bar{I}_1\frac{\partial^2}{\partial t^2}$$

$$L_{34} = \left[-A_{55} + \frac{B_{12}}{R}\right]\frac{\partial}{\partial z} + \left[\frac{\hat{B}_{26}}{R^2} - \frac{A_{45}}{R}\right]\frac{\partial}{\partial\varphi},$$

$$L_{35} = \left[-A_{45} + \frac{B_{26}}{R}\right]\frac{\partial}{\partial z} + \left[\frac{\hat{B}_{22}}{R^2} - \frac{A_{44}}{R}\right]\frac{\partial}{\partial\varphi},$$

$$L_{44} = -\bar{A}_{55} + \bar{D}_{11}\frac{\partial^2}{\partial z^2} + \frac{2D_{16}}{R}\frac{\partial}{\partial z\partial\varphi} + \frac{\hat{D}_{66}}{R^2}\frac{\partial^2}{\partial\varphi^2} - \bar{I}_3\frac{\partial^2}{\partial t^2}$$

$$L_{45} = -A_{45} + \bar{D}_{16}\frac{\partial^2}{\partial z^2} + \frac{D_{12}+D_{66}}{R}\frac{\partial}{\partial z\partial\varphi} + \frac{\hat{D}_{26}}{R^2}\frac{\partial^2}{\partial\varphi^2},$$

$$L_{55} = -\hat{A}_{44} + \bar{D}_{66}\frac{\partial^2}{\partial z^2} + \frac{2D_{26}}{R}\frac{\partial^2}{\partial z\partial\varphi} + \frac{\hat{D}_{22}}{R^2}\frac{\partial^2}{\partial\varphi^2} - \bar{I}_3\frac{\partial^2}{\partial t^2},$$

$$L_{ij} = L_{ji}, \qquad \text{(A-1)}$$

$$\left.\begin{aligned} \bar{A}_{ij} &= A_{ij} + \frac{B_{ij}}{R} \quad \hat{A}_{ij} = A_{ij} - \frac{B_{ij}}{R} \\ \bar{B}_{ij} &= B_{ij} + \frac{D_{ij}}{R} \quad \hat{B}_{ij} = B_{ij} - \frac{D_{ij}}{R} \\ \bar{D}_{ij} &= D_{ij} + \frac{E_{ij}}{R} \quad \hat{D}_{ij} = D_{ij} - \frac{E_{ij}}{R} \end{aligned}\right\} \quad i,j = 1,2,4,5,6$$

(A-2)

Appendix B

Governing equations of thin laminated composite shells

According to Kirchhoff hypothesis of neglecting shear deformation and the assumption that the ε_z is negligible, for laminated composite shell the mid-surface strain and curvature changes as follows:

$$\varepsilon_{0\alpha} = \frac{\partial u}{\partial\alpha},$$

$$\varepsilon_{0\beta} = \frac{\partial v}{\partial\beta} + \frac{w}{R},$$

$$\gamma_{0\alpha\beta} = \frac{\partial v}{\partial\alpha} + \frac{\partial u}{\partial\beta},$$

$$k_\alpha = -\frac{\partial^2 w}{\partial\alpha^2},$$

$$k_\beta = \frac{\partial}{\partial\beta}\left(\frac{v}{R}\right) - \frac{\partial^2 w}{\partial\beta^2},$$

$$\tau = \frac{\partial}{\partial\alpha}\left(\frac{v}{R}\right) - 2\frac{\partial^2 w}{\partial\beta\partial\alpha}, \qquad \text{(B-1)}$$

where, $\{u, v, w\}$ are the displacements of the shell at the neutral surface in the axial, circumferential and radial directions respectively. The forces N and moments M resultant, obtained by integrating the stresses over the shell thickness, are:

$$\begin{bmatrix} N_\alpha \\ N_\beta \\ N_{\alpha\beta} \\ M_\alpha \\ M_\beta \\ M_{\alpha\beta} \end{bmatrix} = \begin{bmatrix} A_{11} & A_{12} & A_{16} & B_{11} & B_{12} & B_{16} \\ A_{12} & A_{22} & A_{26} & B_{12} & B_{22} & B_{26} \\ A_{16} & A_{26} & A_{66} & B_{16} & B_{26} & B_{66} \\ B_{11} & B_{12} & B_{16} & D_{11} & D_{12} & D_{16} \\ B_{12} & B_{22} & B_{26} & D_{12} & D_{22} & D_{26} \\ B_{16} & B_{26} & B_{66} & D_{16} & D_{26} & D_{66} \end{bmatrix} \begin{bmatrix} \varepsilon_{0\alpha} \\ \varepsilon_{0\beta} \\ \gamma_{0\alpha\beta} \\ k_\alpha \\ k_\beta \\ \tau \end{bmatrix}.$$

(B-2)

Equations of motion of a laminated composite thin cylindrical shell in cylindrical coordinate as follows:

$$\frac{\partial N_z}{\partial z} + \frac{1}{R}\frac{\partial N_{z\theta}}{\partial z\partial\theta} + q_z = -\bar{I}\frac{\partial^2 u}{\partial t^2}, \qquad \text{(B-3)}$$

$$\frac{1}{R}\frac{\partial N_\theta}{\partial \theta}+\frac{\partial N_{z\theta}}{\partial z}+\frac{1}{R}\left[\frac{1}{R}\frac{\partial M_\theta}{\partial \theta}+\frac{\partial M_{z\theta}}{\partial z}\right]+q_\theta=-\bar{I}\frac{\partial^2 v}{\partial t^2}, \tag{B-4}$$

$$-\frac{N_\theta}{R}+\frac{\partial^2 N_z}{\partial z^2}+\frac{2}{R}\frac{\partial^2 M_{z\theta}}{\partial z\partial\theta}+\frac{1}{R}\left[\frac{1}{R}\frac{\partial M_\theta}{\partial\theta}+\frac{\partial M_{z\theta}}{\partial z}\right]+q_\xi=-\bar{I}\frac{\partial^2 w}{\partial t^2}. \tag{B-5}$$

The equation of motion can be written in terms of displacements as:

$$L_{ij}\ u_i + M_{ij}\ddot{u}_i = q, \tag{B-6}$$

Where,

$$u_i=[u,\ v,\ w\ ]^T, \tag{B-7}$$

$$M_{ij}=\begin{cases}\bar{I} & i=j\\ 0 & j\neq j\end{cases}, \tag{B-8}$$

$$q=\left[0,0,\left(p_1^I+p_1^R\right)-p_3^T\right]^T. \tag{B-9}$$

The L_{ij} coefficients are given as:

$$L_{11}=A_{11}\frac{\partial^2}{\partial z^2}+2\frac{A_{16}}{R}\frac{\partial^2}{\partial z\partial\varphi}+\frac{A_{66}}{R^2}\frac{\partial^2}{\partial\varphi^2},$$

$$L_{12}=\bar{A}_{16}\frac{\partial^2}{\partial z^2}+\frac{\bar{A}_{12}}{R}\frac{\partial^2}{\partial z\partial\varphi}+\frac{\bar{A}_{26}}{R^2}\frac{\partial^2}{\partial\varphi^2},$$

$$L_{13}=A_{12}^*\frac{\partial}{\partial z}+\frac{A_{26}^*}{R}\frac{\partial}{\partial\varphi}-B_{11}\frac{\partial^3}{\partial z^3}$$
$$-3\frac{B_{16}}{R}\frac{\partial^3}{\partial z^2\partial\varphi}-\frac{B_{17}}{R^2}\frac{\partial^3}{\partial z\partial\varphi^2}-\frac{B_{26}}{R^3}\frac{\partial^3}{\partial\varphi^3},$$

$$L_{22}=A'_{66}\frac{\partial^2}{\partial z^2}+2\frac{A'_{26}}{R}\frac{\partial^2}{\partial z\partial\varphi}+\frac{A'_{22}}{R^2}\frac{\partial^2}{\partial\varphi^2},$$

$$L_{23}=\bar{A}_{26}^*\frac{\partial}{\partial z}+\frac{\bar{A}_{22}^*}{R}\frac{\partial}{\partial\varphi}-\bar{B}_{16}\frac{\partial^3}{\partial z^3}$$
$$-\frac{\bar{B}_{17}}{R}\frac{\partial^3}{\partial z^2\partial\varphi}-3\frac{\bar{B}_{26}}{R^2}\frac{\partial^3}{\partial z\partial\varphi^2}-\frac{\bar{B}_{22}}{R^3}\frac{\partial^3}{\partial\varphi^3},$$

$$L_{33}=\frac{A_{22}^*}{R}-2B_{12}^*\frac{\partial^2}{\partial z^2}-\frac{4B_{26}^*}{R}\frac{\partial^2}{\partial z\partial\varphi}$$
$$-2\frac{B_{22}^*}{R^2}\frac{\partial^2}{\partial\varphi^2}+D_{11}\frac{\partial^4}{\partial z^4}+4\frac{D_{16}}{R}\frac{\partial^4}{\partial z^3\partial\varphi}$$
$$+2\frac{D_{17}}{R^2}\frac{\partial^4}{\partial z^2\partial\varphi^2}+4\frac{D_{26}}{R^3}\frac{\partial^4}{\partial z\partial\varphi^3}\frac{D_{17}}{R^4}\frac{\partial^4}{\partial\varphi^4}$$

$$L_{ij}=L_{ji}, \tag{B-10}$$

$$\bar{A}_{12}=A_{12}+\frac{B_{12}}{R}+A_{66}+\frac{D_{66}}{R},$$

$$\bar{A}_{ij}=A_{ij}+\frac{B_{ij}}{R}\qquad (ij=16,22,26,66),$$

$$B_{17}=B_{12}+2B_{66},$$

$$D_{17}=D_{12}+2D_{66},$$

$$\bar{B}_{ij}=B_{ij}+\frac{D_{ij}}{R}\qquad (ij=16,17,22,26,66),$$

$$A'_{ij}=\bar{A}_{ij}+\frac{\bar{B}_{ij}}{R}\qquad (ij=22,26,66),$$

$$(A_{ij}^*,B_{ij}^*)=\left(\frac{A_{ij}}{R},\frac{B_{ij}}{R}\right),$$

$$(\bar{A}_{ij}^*,\bar{B}_{ij}^*)=\left(\frac{\bar{A}_{ij}}{R},\frac{\bar{B}_{ij}}{R}\right). \tag{B-11}$$

References

1. Smith, P.W. "Sound Transmission Through Thin Cylindrical Shells", J. Acoustical Society of America, Vol. 29, No.6, pp. 721-729, 1957.
2. White, P. "Sound Transmission through a Finite, Closed, Cylindrical Shell", J. Acoustical Society of America, Vol. 40, No. 5 pp. 1124- 1130, 1966.
3. Koval, L.R. "On Sound Transmission into a Thin Cylindrical Shell under Flight Conditions", J. Sound and Vibration, Vol. 48, No.2, pp. 265-275, 1976.
4. Koval, L.R. "On Sound Transmission into an Orthotropic Shell", J. Sound and Vibration Vol. 63, No.1, pp. 51-59, 1979.
5. Koval, L.R. "Sound Transmission into a Laminated Composite Cylindrical Shell", J. Sound and Vibration, Vol. 71, No. 4, pp. 523-530, 1980.
6. Blaise, A., Lesueur C., Gotteland M., Barbe M. "On Sound Transmission into an Orthotropic Infinite Shell: Comparison with Koval Result and Understanding of Phenomena", J. Sound and Vibration, Vol. 150, No.2, pp.233-243, 1991.
7. Blaise, A. and Lesueur, C., "Acoustic Transmission Through a 2-D Orthotropic Multi-layered Infinite Cylindrical Shell", J. Sound and Vibration, Vol. 155, No. 1, pp. 95-109, 1992.
8. Lee, J.H. and Kim, J. "Study on Sound Transmission Characteristics of a Cylindrical Shell Using Analytical and Experimental Models", Applied Acoustic, Vol. 64, No.6, pp. 611-632, 2003.
9. Roussos, L.A., Powell, C. R., Grosveld, F. W. and Koval, L.R. "Noise Transmission Characteristics of Advanced Composite Structure Materials", J. Aircraft, Vol. 21, No.7, pp. 528-835, 1984.

10. Tang, Y.Y., Robinson J.H. and Silcox R.J. "Sound Transmission Through a Cylindrical Sandwich Shell with Honeycomb Core", The 34th AIAA Aerospace Science Meeting and Exhibit (AIAA-96-0877), Vol. 1, Reno, Newvada, 1996.
11. Howe, M.S. "Acoustics of Fluid-Structure Interaction", Cambridge University Press, 2000.
12. Fahy, F. "Sound and Structural Vibration: Radiation, Transmission and Response", Academic Press, New York, NY, 1985.
13. Qatu, M.S. "Vibration of Laminated Shells and Plates", Elsevier Academic Press, 2004.
14. Reddy, J.N. "Mechanics of Laminated Composite Plates and Shells", Theory and Analysis, CRC Press, Second Edition, 2004.
15. Leissa, A. "Vibration of Shells", NASA sp 288 Washington D.C., 1973.
16. Soedel, W. "Vibrations of Shells and Plates", New York, Marcel Dekker Inc., 1993.
17. Pierce, A.D. "Acoustics", McGraw-Hill ,New York, 1981.
18. Mclachlan, N.W. "Bessel Function for Engineers", Oxford University Press, Second Edition, 1955.
19. Norton and M., Karczub, D. "Fundamentals of Noise and Vibration Analysis for Engineers", Cambridge University Press, Second Ed., 2003.
20. Gerald F. and Wheatley, P. O. "Applied Numerical Analysis", Addison-Wesley, 1997.
21. Beranek, L.L. and Ver I.L. "Noise and Vibration Control Engineering", John Wiley and Sons Inc, New York, 1992.